Oxygen Reduction Reaction | Hot Paper

DOI: 10.1002/ange.201406695

Oxygen Reduction Reaction in a Droplet on Graphite: Direct Evidence that the Edge Is More Active than the Basal Plane**

Anli Shen, Yuqin Zou, Qiang Wang, Robert A. W. Dryfe, Xiaobing Huang, Shuo Dou, Liming Dai, and Shuangyin Wang**

Abstract: *Carbon-based metal-free electrocatalysts for the oxygen reduction reaction (ORR) in alkaline medium have been extensively investigated with the aim of replacing the commercially available, but precious platinum-based catalysts. For the proper design of carbon-based metal-free electrocatalysts for the ORR, it would be interesting to identify the active sites of the electrocatalyst. The ORR was now studied with an air-saturated electrolyte solution droplet (diameter ca. 15 μm), which was deposited at a specified position either on the edge or on the basal plane of highly oriented pyrolytic graphite. Electrochemical measurements suggest that the edge carbon atoms are more active than the basal-plane ones for the ORR. This provides a direct way to identify the active sites of carbon materials for the ORR. Ball-milled graphite and carbon nanotubes with more exposed edges were also prepared and showed significantly enhanced ORR activity. DFT calculations elucidated the mechanism by which the charged edge carbon atoms result in the higher ORR activity.*

The oxygen reduction reaction (ORR) is a key process in fuel cells and metal–air batteries. However, the poor reaction kinetics of the ORR have significantly limited the commercialization of fuel cells and metal–air batteries.[1] With different electrocatalysts, the ORR process could proceed either through an efficient four-electron pathway or a less efficient two-step, two-electron pathway.[2] A direct four-electron ORR would lead to high-performance fuel cells and metal–air batteries. Industrially, the most commonly used electrocatalysts for the ORR are precious platinum-based nanomaterials.[3] However, such electrocatalysts, which are derived from precious-metal resources that suffer from limited availability and high costs, exhibit less than ideal kinetics for the ORR, susceptibility to fuel crossover, and poor stability, which have tremendously limited the development and application of such systems.[1b,4] Alternatively, numerous studies have been performed to design and prepare metal-free or precious-metal-free electrocatalysts with comparable electrocatalytic activity towards the ORR.[5]

Carbon-based materials that are doped with heteroatoms have been extensively investigated as efficient metal-free electrocatalysts for the ORR.[6] Previously, we have successfully prepared nitrogen-doped carbon nanotubes (CNTs), nitrogen-doped graphene, and dual-atom-doped CNTs and graphene as efficient metal-free electrocatalysts for the ORR.[7] Our experimental characterization and theoretical calculations have pointed out that the improved activity of doped carbon materials was attributed to the electron-accepting or electron-donating behavior between heteroatoms and adjacent carbon atoms, which alters the charge distribution on the carbon atoms in the carbon plane. Although the heteroatom-doped carbon materials have shown reasonable activity towards the ORR, the preparation of doped carbon materials usually requires high temperatures or complicated equipment.[8] There is significant need to find a more facile way to alter the charge distribution on the carbon atoms in carbon-based electrocatalysts.[9] To find a general principle for the design of efficient metal-free electrocatalysts for the ORR, a fundamental understanding of the ORR activity of these carbon materials is crucial.

Herein, we tried to identify the active sites in graphite and provide direct evidence that the edge of graphite is more active than the basal plane for the ORR. In the present work, a micro apparatus was developed and used for electrochemical studies on the oxygen reduction reaction with highly oriented pyrolytic graphite (HOPG) as the working electrode. An air-saturated droplet with a diameter of approximately 15 μm was deposited at a specified location on the HOPG surface using a microinjection system. The ORR was studied with the HOPG as the working electrode, the air-saturated droplet as the electrolyte, and the Pt wire and a Ag/AgCl wire in a capillary tube connected with the droplet as the counter and reference electrode, respectively.[10] With this technique,

[*] A. Shen,[+] S. Dou, Prof. S. Wang
State Key Laboratory of Chem/Bio-Sensing and Chemometrics
College of Chemistry and Chemical Engineering, Hunan University
Yuelushan, Changsha, Hunan, 410082 (P.R. China)
E-mail: shuangyinwang@hnu.edu.cn
Y. Zou,[+] Prof. R. A. W. Dryfe
School of Chemistry, The University of Manchester
Manchester, M13 9PL (UK)
Prof. Q. Wang
Department of Applied Chemistry, Nanjing Tech University
Nanjing, 211816 (China)
Prof. X. Huang
College of Chemistry and Chemical Engineering
Hunan University of Arts and Science, Changde
Hunan Province (P.R. China)
Prof. L. Dai
Department of Macromolecular Science and Engineering
Case Western Reserve University
Cleveland, OH 44106 (USA)
E-mail: liming.dai@case.edu
[+] These authors contributed equally to this work.

[**] We acknowledge support from AFOSR MURI (FA9550-12-1-0037), the National Science Foundation (IIP-1343270 and CMMI-133123), the Youth 1000 Talent Program of China, and the Inter-discipline Research Program of Hunan University.

Supporting information for this article is available on the WWW under http://dx.doi.org/10.1002/anie.201406695.

we could deposit the air-saturated droplet at any specified location on the HOPG surface to investigate the ORR activity at different locations. Particularly, we compared the ORR activities of the edge and the basal plane of HOPG and found that the edge is much more active than the basal plane. The conclusion that the edge is much more active than the basal plane of graphite led us to design a bulk graphite powder with enriched edges as an efficient metal-free electrocatalyst for the ORR. The graphite powder, which was prepared by ball-milling, indeed showed significantly enhanced catalytic activity for the ORR.[11] DFT calculations were also performed to investigate the effect of the edge carbon atoms, confirming that the higher charge densities on the edge carbon atoms contributed to the improved catalytic activity for the ORR. This work clearly indicates where the active sites are on graphite for the ORR.

Figure 1 a illustrates how the ORR testing was carried out at specified locations on HOPG. The ORR testing was performed inside a deposited droplet of aqueous KOH solution (1M) on the specimen surface using a micromanipulator–microinjection system, which consisted of a micropipette held by a motorized manipulator (Siskiyou MX7630) and was connected to the micro-injector (PV820 Pneumatic PicoPump, WPI) by the pipette holder with suitable Luer fittings. It should be pointed out that a KOH solution with a concentration of 1M was used instead of the typically used 0.1M KOH solution for ORR testing in alkaline medium to minimize the immediate evaporation of such small droplets. Two representative locations on the HOPG were selected for ORR testing: the edge (Figure 1 b) and the basal plane (Figure 1 c). It could be observed that the air-saturated droplet (diameter: 15 μm) was precisely deposited at the specified location. Once the droplet had been deposited at the specified location, linear sweep voltammetry (LSV) was performed at a scan rate of $10\,mV\,s^{-1}$ (Figure 1 d). The current obtained by the LSV was normalized by the area that the droplet covered to reflect the real activity ($mA\,cm^{-2}$) for the ORR (Figure 1 d). It can be seen that the ORR on the edge proceeded with a more positive onset potential (where the ORR commences) and a higher current density than that on the basal plane of HOPG, indicating that the edge of graphite is more active than the basal plane. We also studied the ORR by depositing the air-saturated droplet at various different locations and obtained similar results. However, once the working electrode area that the droplet covered had comparatively fewer edges, the ORR activity difference between the edge and the basal plane would be very small, as shown in the Supporting Information, Figure S1. These results provide direct evidence that the edge is more active than the basal plane of graphite for ORR, and that the activity is strictly related to the fraction of edges present in the graphite. This conclusion could provide a general principle for the design of efficient carbon-based metal-free electrocatalysts for ORR. It is expected that carbon materials with more exposed edges may show efficient electrocatalytic activity for ORR. To validate this hypothesis, we prepared a series of ball-milled graphite materials with more exposed edges and investigated their electrocatalytic activities for the ORR, as discussed below.

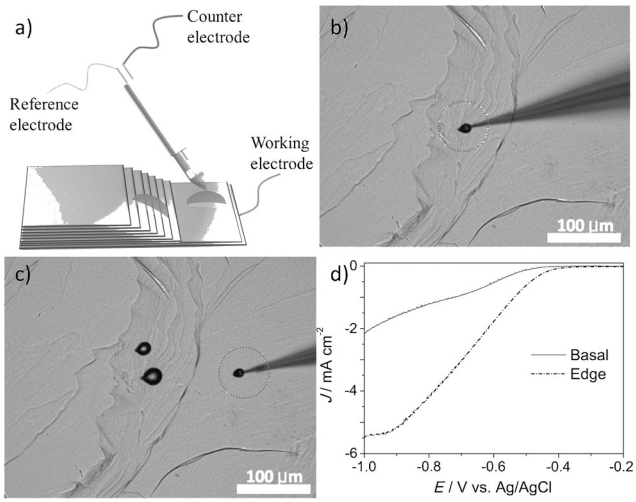

Figure 1. a) Micro apparatus for the ORR electrochemical experiment. b) Optical photograph of the HOPG as the working electrode with the air-saturated droplet deposited on the edge of the HOPG. c) The air-saturated droplet was deposited on the basal plane of the HOPG electrode. d) LSV curves of the ORR tested for a droplet located either on the edge (as shown in Figure 1 b) or on the basal plane (as shown in Figure 1 c) of the HOPG.

We chose a commercial graphite material (100 mesh) as the starting point for the subsequent ball-milling treatment for different periods of time (0–96 h). Figure 2 shows the scanning electron microscopy (SEM) images of graphite materials that had been ball-milled for different periods of time. Obviously, with increasing ball-milling time, the average

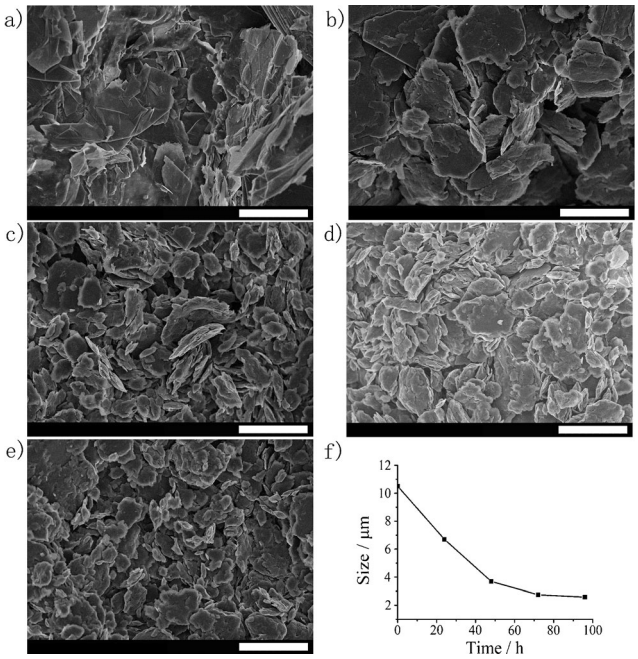

Figure 2. a–e) SEM images of graphite material that had been ball-milled for 0 (a), 24 (b), 48 (c), 72 (d), and 96 hours (e). f) Dependence of the average particle size of the graphite on the duration of the ball-milling process. Scale bars: 10.0 μm.

particle size decreased gradually (as shown in Figure 2 f), implying that more and more edges were exposed after ball-milling. Raman spectroscopy was used to monitor the change in the electronic structure of graphite with ball-milling time (Figure S2). The intensity ratio between the D band and the G band was used as an indicator of the edge/defect ratio of the carbon material. Upon ball-milling, the I_D/I_G ratio showed an apparent increase from 0.19 for pristine graphite to 1.12 for graphite that had been ball-milled for 96 hours, and the ratio increased gradually with the ball-milling time. The Raman characterization indicated that more and more edges were exposed with increased ball-milling time.

Electrochemical characterizations were performed to investigate the ORR activity of the ball-milled graphite to understand how the exposed edges affected the catalytic activity. The cyclic voltammograms (CVs) obtained at a scan rate of 50 mV s^{-1} in O_2- or N_2-saturated 0.1 M KOH solution on graphite are shown in Figure 3. With the O_2-saturated 0.1 M KOH solution, clear oxygen reduction peaks were observed

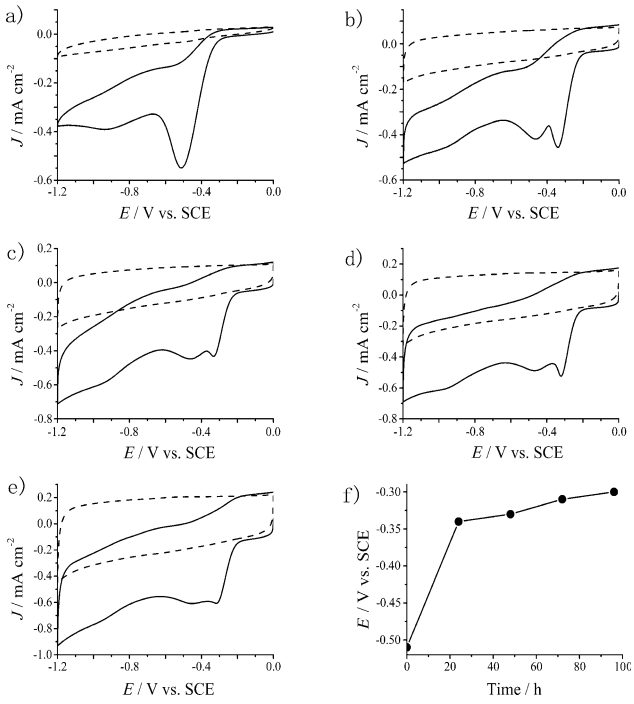

Figure 3. a–e) CV curves of graphite that had been ball-milled for 0 (a), 24 (b), 48 (c), 72 (d), and 96 hours (e) in nitrogen- (– – –) or oxygen-saturated (——) aqueous KOH electrolyte solutions (0.1 M). Scan rate: 50 mV s^{-1}.

for all of the graphite electrodes, but not with the N_2-saturated solution. For the ORR, the CV curve of pristine graphite showed a reduction peak potential of −0.51 V. Upon ball-milling, the reduction peak potential of the ORR shifted towards positive values (Figure 3 f), and this trend is similar to the decrease in the average particle size (Figure 2 f) and to the increase in the I_D/I_G ratio observed by Raman spectroscopy (Figure S2). In particular, graphite that had been ball-milled for 96 hours (denoted as G100-BM-96) showed the most positive reduction peak potential, confirming that G100-BM-96, which features more exposed edges than pristine graphite, is much more active. To further investigate the ORR performance and its kinetic properties, we performed linear sweep voltammetry (LSV) measurements on a rotating disk electrode (RDE) with the graphite cast as the working electrodes. As shown in Figure S3, the ORR process on the pristine graphite electrode commenced at around −0.30 V (onset potential), whereas the ORR onset potential of the ball-milled graphite significantly shifted towards more positive values with an increase in ball-milling time. Meanwhile, the diffusion current density also increased gradually. Similar to the CV observations in Figure 3 f, the LSV curves also demonstrated that the ORR activity of graphite increased with an increase in ball-milling time, as shown in Figure S3 f.

Of all the ball-milled graphite materials, G100-BM-96 showed the best ORR electrocatalytic activity. To fully understand why the ball-milled graphite showed higher ORR activity, we performed more extensive physical and electrochemical characterizations of G100-BM-96 and pristine graphite to relate the structural properties to their electrocatalytic activity. X-ray photoelectron spectroscopy was used to identify the chemical states of pristine graphite and G100-BM-96. Figure S4 shows the XPS spectra of pristine graphite and G100-BM-96. For the C1 s spectra in Figure S4a, it could be found that the full width at half maximum for G100-BM-96 is wider than that for pristine graphite, indicating that more edges are exposed by the ball-milling process.[12] Rotating ring disk electrode (RRDE) testing was performed to confirm the electron transfer number of the ORR on pristine graphite and G100-BM-96. As shown in Figure 4 a,

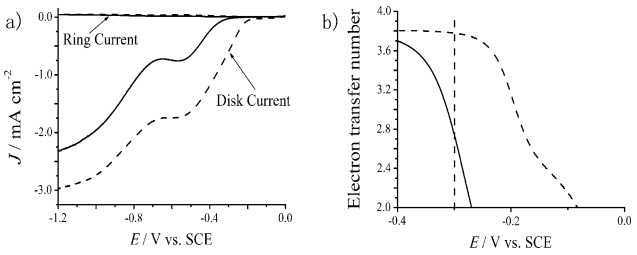

Figure 4. a) RRDE experiments with pristine graphite and G100-BM-96 in O_2-saturated KOH electrolyte solution (0.1 M.). b) The dependence of the electron transfer number on the potential. – – –: 96 hours; ——: 0 hours.

similar to the results of the RDE experiments, the LSV curves obtained by the RRDE testing also confirmed that G100-BM-96 was more active than pristine graphite in terms of its onset potential and the diffusion current density. The dependence of the electron transfer number per O_2 molecule (n), as calculated according to Eq. S1, on the potential is plotted for pristine graphite and G100-BM-96 in Figure 4 b. Clearly, G100-BM-96 shows a significantly higher electron transfer number in the kinetic potential region of the ORR. As the electron transfer number of the ORR is higher for ball-milled graphite than for pristine graphite, it can be deduced that the reaction kinetics of the ORR are more efficient on ball-milled graphite with more edges exposed. On the other hand, the kinetic current density of the ORR could mostly reflect the

intrinsic catalytic activity of the electrode materials.[13] According to the Koutecký–Levich equation [Eq. (S2)],[2a,14] the kinetic current densities at a potential of −0.4 V were calculated to be 0.25 and 2.15 mA cm^{-2} for pristine graphite and G100-BM-96, respectively, confirming that the ball-milled graphite is more active than pristine graphite in the ORR. It is worth noting that the ball-milling process would generate more edges as well as a higher surface area for the ball-milled graphite. Indeed, for ball-milled graphite, larger Brunauer—Emmett—Teller (BET) surface areas were measured (Figure S5). To more precisely investigate the contribution of the exposed edges, the kinetic current at −0.4 V was normalized by the BET surface area to obtain the true kinetic current densities of the graphite material per BET surface area (mA cm$_{BET}^{-2}$). After the normalization, the kinetic current density of the ORR on ball-milled G100-BM-96 was 2.5 times higher than that for pristine graphite (0.047 vs. 0.019 mA cm$_{BET}^{-2}$). The higher normalized kinetic current density of G100-BM-96 reflects the true contribution of the edges to the enhanced ORR activity (Figure S6). Besides, the efficient G100-BM-96 catalyst also showed excellent methanol tolerance and durability in the ORR, as discussed in the Supporting Information (Figure S7 and Figure S8).

The ball-milling strategy to improve the ORR activity of graphite materials also applies to other carbon materials. For example, we also used the ball-milling approach to treat carbon nanotubes (CNTs). The Raman spectra of CNT before and after the ball-milling treatment confirmed the presence of more edges after the ball-milling process (Figure S9). Electrochemical LSV characterization, as shown in Figure S10, also demonstrated that ball-milled CNT is more active than pristine CNT for the ORR. Therefore, the conclusion that the edge is more active than the basal plane for the ORR also applies to other carbon materials. More directly, we compared the ORR activity of commercial graphite with different average particle sizes to determine how the edges affect its performance. Indeed, electrochemical experiments confirmed that graphite with smaller particle sizes shows higher ORR activity (Figure S11–S13).

The physical and electrochemical characterization of the bulk powder graphite materials successfully validated the conclusion based on the results of the ORR on the electrochemical micromanipulator/microinjection system, confirming that the edge of graphite is more active than the basal plane. Finally, to unveil the mechanism of this activity difference, we performed DFT calculations on a graphene model (Figure S14) to study the charge distribution on the carbon atoms. It was found that the basal-plane carbon atoms carry negligible charge (Figure S14). However, higher charge densities were observed on the edge carbon atoms. According to Xia's report[9] and our previous work,[7b] the carbon atoms with higher charge densities are more likely to serve as catalytically active sites. Therefore, the edge carbon atoms of graphene with higher charge densities could provide more active sites than the basal-plane carbon atoms to catalyze ORR. Therefore, the as-observed higher ORR activity of the edge carbon atoms could be attributed to the higher charge density on the edge carbon atoms, resulting in enhanced ORR activity.

In summary, by studying the ORR reaction in an air-saturated micro-droplet at a specified location either on the edge or on the basal plane of HOPG using the electrochemical micromanipulator–microinjection system, we provide the first direct evidence that the edge of the carbon materials is more active than the basal plane for the ORR, which is in contrast with Unwin's work.[15] To validate this finding, we successfully prepared bulk graphite powder with controlled edges by a ball-milling method. Our physical and electrochemical results confirm that the ball-milled graphite with more exposed edges shows a much better electrocatalytic performance for the ORR. This ball-milling strategy also applies to other carbon materials, such as carbon nanotubes. Our DFT calculations demonstrated that the higher ORR activity of the edge carbon atoms originates from the delocalized charge distribution on the edge carbon atoms.[16]

Received: June 30, 2014
Published online: August 14, 2014

Keywords: droplets · electrochemistry · fuel cell · graphite · oxygen reduction reaction

[1] a) K. Gong, F. Du, Z. Xia, M. Durstock, L. Dai, *Science* **2009**, *323*, 760 – 764; b) L. Qu, Y. Liu, J.-B. Baek, L. Dai, *ACS Nano* **2010**, *4*, 1321 – 1326; c) J. Xu, W. Huang, R. L. McCreery, *J. Electroanal. Chem.* **1996**, *410*, 235 – 242.

[2] a) S. Wang, D. Yu, L. Dai, *J. Am. Chem. Soc.* **2011**, *133*, 5182 – 5185; b) M. Dudek, M. Sitarz, P. Tomczyk, *J. Solid State Electrochem.* **2014**, *0*, 0.

[3] a) S. Guo, S. Sun, *J. Am. Chem. Soc.* **2012**, *134*, 2492 – 2495; b) W. Ding, Z. Wei, S. Chen, X. Qi, T. Yang, J. Hu, D. Wang, L. J. Wan, S. F. Alvi, L. Li, *Angew. Chem.* **2013**, *125*, 11971 – 11975; *Angew. Chem. Int. Ed.* **2013**, *52*, 11755 – 11759.

[4] a) S. Yang, X. Feng, X. Wang, K. Müllen, *Angew. Chem.* **2011**, *123*, 5451 – 5455; *Angew. Chem. Int. Ed.* **2011**, *50*, 5339 – 5343; b) J. Liang, Y. Jiao, M. Jaroniec, S. Z. Qiao, *Angew. Chem.* **2012**, *124*, 11664 – 11668; *Angew. Chem. Int. Ed.* **2012**, *51*, 11496 – 11500.

[5] a) Y. Zheng, Y. Jiao, J. Chen, J. Liu, J. Liang, A. Du, W. Zhang, Z. Zhu, S. C. Smith, M. Jaroniec, G. Q. Lu, S. Z. Qiao, *J. Am. Chem. Soc.* **2011**, *133*, 20116 – 20119; b) X. Sun, Y. Zhang, P. Song, J. Pan, L. Zhuang, W. Xu, W. Xing, *ACS Catal.* **2013**, *3*, 1726 – 1729.

[6] a) D. Yu, Y. Xue, L. Dai, *J. Phys. Chem. Lett.* **2012**, *3*, 2863 – 2870; b) Y. Su, Y. Zhang, X. Zhuang, S. Li, D. Wu, F. Zhang, X. Feng, *Carbon* **2013**, *62*, 296 – 301; c) Y. Zhang, X. Zhuang, Y. Su, F. Zhang, X. Feng, *J. Mater. Chem. A* **2014**, *2*, 7742; d) W. Wei, H. Liang, K. Parvez, X. Zhuang, X. Feng, K. Müllen, *Angew. Chem.* **2014**, *126*, 1596 – 1600; *Angew. Chem. Int. Ed.* **2014**, *53*, 1570 – 1574.

[7] a) X. Wang, J. Wang, D. Wang, S. Dou, Z. Ma, J. Wu, L. Tao, A. Shen, C. Ouyang, Q. Liu, S. Wang, *Chem. Commun.* **2014**, *50*, 4839 – 4842; b) S. Wang, L. Zhang, Z. Xia, A. Roy, D. W. Chang, J. B. Baek, L. Dai, *Angew. Chem.* **2012**, *124*, 4285 – 4288; *Angew. Chem. Int. Ed.* **2012**, *51*, 4209 – 4212; c) S. Wang, E. Iyyamperumal, A. Roy, Y. Xue, D. Yu, L. Dai, *Angew. Chem.* **2011**, *123*, 11960 – 11964; *Angew. Chem. Int. Ed.* **2011**, *50*, 11756 – 11760.

[8] a) C. N. R. Rao, R. Voggu, *Mater. Today* **2010**, *13*, 34 – 40; b) L. Dai, *Acc. Chem. Res.* **2013**, *46*, 31 – 42.

[9] a) L. Zhang, J. Niu, M. Li, Z. Xia, *J. Phys. Chem. C* **2014**, *118*, 3545 – 3553; b) L. Zhang, Z. Xia, *J. Phys. Chem. C* **2011**, *115*, 11170 – 11176.

[10] a) C. E. Banks, T. J. Davies, G. G. Wildgoose, R. G. Compton, *Chem. Commun.* **2005**, 829 – 841; b) P. S. Toth, A. T. Valota, M. Velický, I. A. Kinloch, K. S. Novoselov, E. W. Hill, R. A. W. Dryfe, *Chem. Sci.* **2014**, *5*, 582; c) I.-Y. Jeon, S. Zhang, L. Zhang, H.-J. Choi, J.-M. Seo, Z. Xia, L. Dai, J.-B. Baek, *Adv. Mater.* **2013**, *25*, 6138 – 6145; d) I. Y. Jeon, H. J. Choi, S. M. Jung, J. M. Seo, M. J. Kim, L. Dai, J. B. Baek, *J. Am. Chem. Soc.* **2013**, *135*, 1386 – 1393; e) I. Y. Jeon, H. J. Choi, M. Choi, J. M. Seo, S. M. Jung, M. J. Kim, S. Zhang, L. Zhang, Z. Xia, L. Dai, N. Park, J. B. Baek, *Sci. Rep.* **2013**, *3*, 1810.

[11] W. Yuan, Y. Zhou, Y. Li, C. Li, H. Peng, J. Zhang, Z. Liu, L. Dai, G. Shi, *Sci. Rep.* **2013**, *3*, 2248.

[12] T. Y. Leung, W. F. Man, P. K. Lim, W. C. Chan, F. Gaspari, S. Zukotynski, *J. Non-Cryst. Solids* **1999**, *254*, 156 – 160.

[13] a) C. Zhang, N. Mahmood, H. Yin, F. Liu, Y. Hou, *Adv. Mater.* **2013**, *25*, 4932 – 4937; b) J. Liang, X. Du, C. Gibson, X. W. Du, S. Z. Qiao, *Adv. Mater.* **2013**, *25*, 6226 – 6231.

[14] Y. Ito, H. J. Qiu, T. Fujita, Y. Tanabe, K. Tanigaki, M. Chen, *Adv. Mater.* **2014**, *26*, 4145.

[15] S. C. S. Lai, A. N. Patel, K. McKelvey, P. R. Unwin, *Angew. Chem.* **2012**, *124*, 5354 – 5354; *Angew. Chem. Int. Ed.* **2012**, *51*, 5260 – 5260.

[16] M. Olivucci, A. Lami, F. Santoro, *Angew. Chem.* **2005**, *117*, 5248 – 5251; *Angew. Chem. Int. Ed.* **2005**, *44*, 5118 – 5121.